Discrete Velocity Numerical Approach to Strong Evaporation of Graphite

A.V. Gusarov

Baikov Institute of Metallurgy, Russian Academy of Sciences
Leninsky Prospekt 49, 119991 Moscow, Russia, E-mail: AV.Gusarov@relcom.ru

Abstract. Carbon vapor formed at graphite evaporation contains considerable amounts of molecules C_2 and C_3 along with single atoms C. A numerical kinetic approach to gas mixtures is proposed which is based on a relaxation model for the Boltzmann equation. It is found that relations between the pressure and temperature ratios and the Mach number behind the Knudsen layer do not depend on vapor composition and are the same as in one-component vapor. The molecular composition of vapor is determined by decreasing the thermal velocity with molecular mass that decreases evaporation rate of heavier species and by decreasing the recondensation fraction with molecular mass that acts oppositely.

INTRODUCTION

Carbon vapor obtained by evaporation of graphite is known to contain considerable fractions of molecules C_2 and C_3 along with single atoms C [1]. Recent experiments on near-threshold laser ablation [2] indicate that the molecules do not form in the gas phase but are ejected directly from the condensed phase. The molecules may act as condensation centers that is very important in gas-phase synthesis of larger clusters [3], fullerens, and single-wall carbon nanotubes [4]. Evaporation rate and molecular composition of vapor both depend on microscopic laws of molecule-condensed phase interaction and on molecular collisions in the Knudsen layer in vapor adjacent to the surface. The present work is devoted to a multicomponent Knudsen layer.

Strong evaporation problem is well studied for one-component vapors [5-7] . Peculiarities arising at evaporation of two-component substrates have been analyzed [7-8] by Direct Simulation Monte Carlo simulation. An approach to binary mixture condensation [9] is known where a relaxation model for gas mixture [10] was numerically studied.

MODEL

Evaporation from a plane condensed-phase surface is considered. Relaxation model [10] is accepted with an N-component gas mixture described by velocity distribution functions f_α satisfying the transport equations:

$$\frac{\partial f_\alpha}{\partial t} + c_z \frac{\partial f_\alpha}{\partial z} = \sum_{\beta=1}^{N} \omega_{\alpha\beta}(F_{\alpha\beta} - f_\alpha) \qquad \text{for } \alpha = 1 \,..\, N, \tag{1}$$

where t is the time, z the coordinate along the normal to the surface, c_z the projection of the molecular velocity to the normal, $\omega_{\alpha\beta}$ the effective collision frequency of a particle of species α with particles of species β, and $F_{\alpha\beta}$ the reference distribution functions. The collision terms satisfy the collisional invariant conditions:

$$\int (F_{\alpha\alpha} - f_\alpha)(1, c_z, c^2)\mathrm{d}\mathbf{c} = 0\,, \tag{2}$$

$$\int (F_{\alpha\beta} - f_\alpha)\mathrm{d}\mathbf{c} = 0\,, \tag{3}$$

$$\omega_{\alpha\beta} m_\alpha \int (F_{\alpha\beta} - f_\alpha)(c_z, c^2)\mathrm{d}\mathbf{c} + \omega_{\beta\alpha} m_\beta \int (F_{\beta\alpha} - f_\beta)(c_z, c^2)\mathrm{d}\mathbf{c} = 0\,, \tag{4}$$

where $\mathbf{c}$ is the vector of molecular velocity, c its absolute value, and m_α the molecular mass of species α. Two additional conditions specific for Maxwell molecules are required [10]:

CP762, *Rarefied Gas Dynamics: 24th International Symposium,* edited by M. Capitelli

Report Documentation Page

Form Approved
OMB No. 0704-0188

1. REPORT DATE	2. REPORT TYPE	3. DATES COVERED
13 JUL 2005	**N/A**	**-**

4. TITLE AND SUBTITLE	5a. CONTRACT NUMBER
Discrete Velocity Numerical Approach to Strong Evaporation of Graphite	5b. GRANT NUMBER
	5c. PROGRAM ELEMENT NUMBER
6. AUTHOR(S)	5d. PROJECT NUMBER
	5e. TASK NUMBER
	5f. WORK UNIT NUMBER
7. PERFORMING ORGANIZATION NAME(S) AND ADDRESS(ES) **Baikov Institute of Metallurgy, Russian Academy of Sciences Leninsky Prospekt 49, 119991 Moscow, Russia**	8. PERFORMING ORGANIZATION REPORT NUMBER
9. SPONSORING/MONITORING AGENCY NAME(S) AND ADDRESS(ES)	10. SPONSOR/MONITOR'S ACRONYM(S)
	11. SPONSOR/MONITOR'S REPORT NUMBER(S)

12. DISTRIBUTION/AVAILABILITY STATEMENT
Approved for public release, distribution unlimited

13. SUPPLEMENTARY NOTES
See also ADM001792, International Symposium on Rarefied Gas Dynamics (24th) Held in Monopoli (Bari), Italy on 10-16 July 2004.

14. ABSTRACT

15. SUBJECT TERMS

16. SECURITY CLASSIFICATION OF:			17. LIMITATION OF ABSTRACT	18. NUMBER OF PAGES	19a. NAME OF RESPONSIBLE PERSON
a. REPORT **unclassified**	b. ABSTRACT **unclassified**	c. THIS PAGE **unclassified**	**UU**	**6**	

$$\int (F_{\alpha\beta} - f_\alpha) c_z \mathrm{d}\mathbf{c} = \frac{m_\beta}{m_\alpha + m_\beta} n_\alpha (u_\beta - u_\alpha)\,, \tag{5}$$

$$\int (F_{\alpha\beta} - f_\alpha)[(c_z - u_\alpha)^2 + c_r^2]\mathrm{d}\mathbf{c} = \frac{2m_\beta}{(m_\alpha + m_\beta)^2} n_\alpha [3k(T_\beta - T_\alpha) + m_\beta (u_\beta - u_\alpha)^2]\,, \tag{6}$$

where c_r is the projection of the molecular velocity to the condensed phase surface, k the Boltzmann constant, and n_α, u_α and T_α are the number density, the average velocity, and the temperature, respectively, of species α.

Discrete Velocity Method

Discrete velocity method [11] is applied for numerical solution of system (1). The two-dimensional velocity space (c_z, c_r) is divided into equal rectangular cells with center coordinates c_z^i and c_r^j, where i and j are integers. The discrete velocity distributions, f_α^{ij}, are defined as averages of f_α over cell (i, j). Approximation of the left-hand side of Eq. (1) by a second-order essentially non-oscillatory scheme is described in [11] while evaluation of the discrete reference distributions $F_{\alpha\beta}^{ij}$ is original in the present work. They are looking for in the following form corresponding to the continuous model [10]:

$$F_{\alpha\beta}^{ij} = \{A_{\alpha\beta} + B_{\alpha\beta}(c_z^i - u) + C_{\alpha\beta}[(c_z^i - u)^2 + (c_r^j)^2]\} \exp\{-\Gamma_\alpha[(c_z^i - \Delta_\alpha)^2 + (c_r^j)^2]\}\,, \tag{7}$$

where u is the mass-averaged velocity of the mixture. Coefficients Γ_α and Δ_α specify equilibrium discrete distributions corresponding to molecular masses, m_α, and temperature, T, and velocity, u, of the mixture. They satisfy the following equations [11]:

$$R_1 = 0\,, \qquad R_2 S_0 + R_0 (S_2 - \frac{3kT}{m_\alpha} S_0) = 0\,, \tag{8}$$

with the sums

$$R_\gamma = \sum_i (c_z^i - u)^\gamma \exp[-\Gamma_\alpha (c_z^i - \Delta_\alpha)^2]\,, \tag{9}$$

$$S_\gamma = \sum_j (c_r^j)^\gamma \exp[-\Gamma_\alpha (c_r^j)^2] w_j\,, \tag{10}$$

where $w_j \sim c_r^j$ is the volume of velocity-space cell (i, j) [11]. Equations (8) are numerically solved by the Newton method with the initial approximations of $\Gamma_\alpha = m_\alpha/(2kT)$ and $\Delta_\alpha = u$, which correspond to the continuous limit.

A discrete approximation of Eqs. (2)-(6) gives the following system of linear equations for each triple, $A_{\alpha\beta}$, $B_{\alpha\beta}$, and $C_{\alpha\beta}$, at any combination of α and β:

$$A_{\alpha\beta} R_0 S_0 + B_{\alpha\beta} R_1 S_0 + C_{\alpha\beta}(R_2 S_0 + R_0 S_2) = n_\alpha\,, \tag{11}$$

$$A_{\alpha\beta} R_1 S_0 + B_{\alpha\beta} R_2 S_0 + C_{\alpha\beta}(R_3 S_0 + R_1 S_2) = n_\alpha (u_{\alpha\beta} - u)\,, \tag{12}$$

$$A_{\alpha\beta}(R_2 S_0 + R_0 S_2) + B_{\alpha\beta}(R_3 S_0 + R_1 S_2) + C_{\alpha\beta}(R_4 S_0 + 2R_2 S_2 + R_0 S_4) = 3n_\alpha kT_{\alpha\beta}/m_\alpha + n_\alpha (u_{\alpha\beta} - u)^2\,, \tag{13}$$

where

$$u_{\alpha\beta} = \frac{m_\alpha u_\alpha + m_\beta u_\beta}{m_\alpha + m_\beta}\,, \qquad T_{\alpha\beta} = T_\alpha + \frac{2m_\alpha m_\beta}{(m_\alpha + m_\beta)^2}[T_\beta - T_\alpha + \frac{m_\beta}{6k}(u_\alpha - u_\beta)^2]\,. \tag{14}$$

Microscopic Characteristics of Carbon Vapor

A three-component mixture of atoms C and molecules C_2 and C_3 is considered. While 4- and 5-atomic molecules are often present in carbon vapor [1-2], their concentrations are negligible and so they are not taken into account. Collisions between molecules may result in changing their vibrational and rotational states and even in their dissociation or merging. Cross-sections of these non-elastic processes are supposed to be considerably less than the elastic collision cross-section. Therefore, non-elastic collisions can be neglected within the Knudsen layer where an evaporated molecule is subjected to few collisions only. Equation (1) actually describes translational degrees of freedom only. Internal states are supposed to be uniform in the Knudsen layer.

To estimate relaxation frequencies $\omega_{\alpha\beta}$, a correlation [11] between the rigid spheres model and the relaxation model is used. In case of mixture, the relaxation frequencies are proportional to the corresponding collision cross-sections $\sigma_{\alpha\beta}$ of molecules α with molecules β:

$$\omega_{\alpha\beta} = \frac{32}{15} n_\beta \sigma_{\alpha\beta} \left(\frac{kT}{\pi \mu_{\alpha\beta}} \right)^{1/2}, \qquad \mu_{\alpha\beta} = \frac{2 m_\alpha m_\beta}{m_\alpha + m_\beta}. \tag{15}$$

The most stable configuration of molecule C_3 is the linear one [12], therefore it is considered as a circular cylinder with hemispherical ends as shown in Fig. 1 (a). The same geometry describes molecules C_2 and atoms C (reduced case with cylinder length equal to zero). The only parameter characterizing size of the molecules is atomic diameter a. This value is taken equal to 2 Angstroms that roughly corresponds to mean interatomic distance in graphite. Cross-sections $\sigma_{\alpha\beta}$ are estimated in assumption that striking molecules can be oriented along the three coordinate axes that gives 9 possible pair combinations, which can be classified as shown in Fig. 1 (b). Averaging over all the orientations gives the mean collision cross-section of a molecule C_α with a molecule C_β:

$$\sigma_{\alpha\beta} = \pi a^2 \{1 + \frac{2}{9\pi} [\alpha\beta + 5(\alpha + \beta) - 11]\} \qquad \text{for } \alpha,\beta = 1, 2, 3. \tag{16}$$

Experimental data concerning interaction of vapor molecules with the condensed phase surface are rather limited [1,2]. Complete sticking of impinging molecules is supposed in the present model that corresponds to the condensation coefficient of 1. Velocity distributions of molecules ejected from the condensed phase are specified by Maxwellians corresponding to surface temperature T_s and partial pressures of components $p_{s\alpha}$ in the saturated vapor:

$$f_\alpha = \frac{p_{s\alpha} / kT_s}{(2\pi kT_s / m_\alpha)^{3/2}} \exp\left(- \frac{m_\alpha \mathbf{c}^2}{2kT_s} \right). \tag{17}$$

RESULTS AND DISCUSSION

Figures 2-3 show detailed calculation results for an example of steady-state evaporation at the pressure ratio $p_a/p_s = 0.22$ where p_a is the ambient pressure far from the Knudsen layer. Equal partial saturated pressures $p_{s1} = p_{s2} = p_{s3} = p_s/3$ are chosen to exhibit peculiarities caused by multicomponent vapor. A strong evaporation flow with the Mach number $M = 0.964$ at infinity is formed at such parameters.

Figure 2 shows profiles of characteristic moments of velocity distribution functions in the Knudsen layer. Dimensionless parameters are used with pressure and temperature normalized by saturated vapor pressure p_s and surface temperature T_s, respectively. Density and velocity are normalized by saturated vapor density $n_s = p_s/kT_s$ and thermal velocity of monatomic carbon vapor at the surface temperature $u_0 = (2kT_s/m_1)^{1/2}$. Net heat flow q in the frame moving with the vapor is measured in the units of $u_0 p_s$. Dimensionless coordinate in this figure is the ratio of distance z from the surface to the mean free path of monatomic carbon vapor at saturated vapor density $l_s = 1/(\pi a^2 n_s)$.

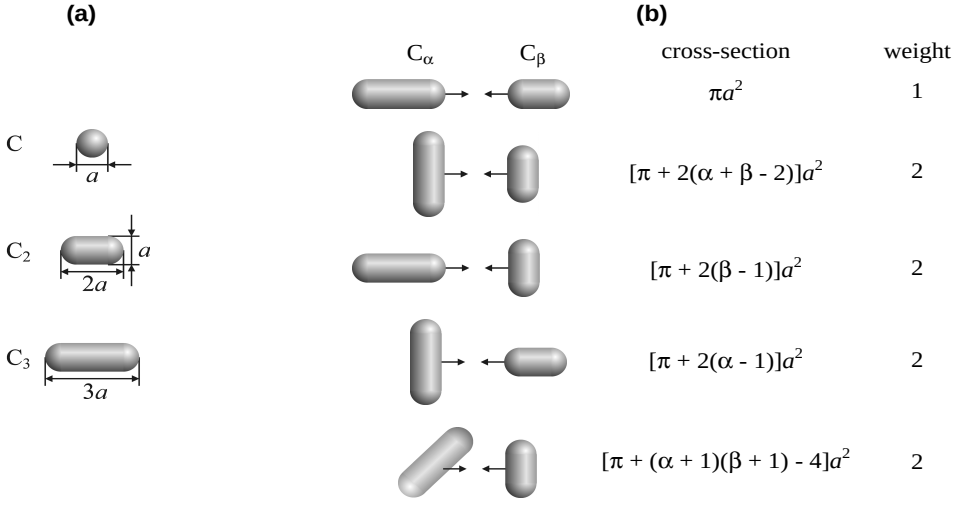

FIGURE 1. Geometric parameters of carbon molecules (a) accepted for estimation collision cross-sections at various mutual orientations of striking molecules C_α and C_β (b). Symbol a designates the carbon atom diameter. Collision cross-sections at particular orientations along with their weights are indicated on the right.

All the parameters shown in Fig. 2 change sharply near the surface but tend to constant values at infinity. Number density of vapor (see broken line in Fig. 2 (c)) and all its components (Fig. 2 (a)) decrease in the Knudsen layer. It should be noted that number densities of carbon vapor species considerably decrease with their molecular masses (see Fig. 2 (a)) while their densities in the saturated vapor are equal in the considered case. The difference in the carbon species transport in the Knudsen layer is clearly seen in Fig. 2 (b) where relative concentrations $x_\alpha = n_\alpha/(n_1 + n_2 + n_3)$ are plotted. The concentration of atoms is higher than the value of 1/3 in the saturated vapor and increases with distance. The concentration of molecules C_2 is about 1/3 and that of molecules C_3 is less than 1/3 and decreases with distance. This can be qualitatively explained by difference in thermal velocities: the lightest monatomic component with the highest thermal velocity evaporates more effectively than the heaviest molecule C_3 with the lowest thermal velocity. Similar result was obtained for two-component vapor [7-8].

Parameters of the multicomponent vapor in the Knudsen layer presented in Fig. 2 (c), (d) are qualitatively the same as for one-component vapor [6,11]. Local Mach number $M = u/c$ (upper full line in Fig. 2 (c)) is defined as the ratio of vapor velocity u to local sound speed $c = [(5/3)\,p/(m_1n_1 + m_2n_2 + m_3n_3)]^{1/2}$, where p is the pressure of the mixture. The last equation for the sound speed is obtained in assumption of no exchange between translational and internal degrees of freedom that corresponds to the accepted kinetic model (1). The local Mach number increases in the Knudsen number and tends to the value of 0.964 at infinity.

Difference between axial, p_{zz} (full line in Fig. 2 (d)), and radial, p_{rr} (broken line), pressure tensor components and deviation of heat flow q (chain line) from zero characterize degree of nonequilibrium that can be used to define thickness of the Knudsen layer [11]. One can see that the layer of "mechanical" nonequilibrium with $p_{zz} \neq p_{rr}$ is thinner than the layer of "thermal" nonequilibrium with $q \neq 0$ as in case of one component [11]. Knudsen layer thickness considerably increases when Mach number at infinity approaches unity as in one component vapor [11].

Figure 3 shows velocity distribution functions of the three components at the surface. The forward part of the velocity distributions is the half-Maxwellian defined by Eq. (17) and the backward part at $c_z < 0$ characterizes back condensation of evaporated species that have changed their directions due to collisions in the Knudsen layer. The backward part is rather sensitive to processes in the Knudsen layer [5-6,11]. A discontinuity at the plane $c_z = 0$ between the forward and backward parts is clearly seen in Fig. 3 that is general for the Knudsen layer.

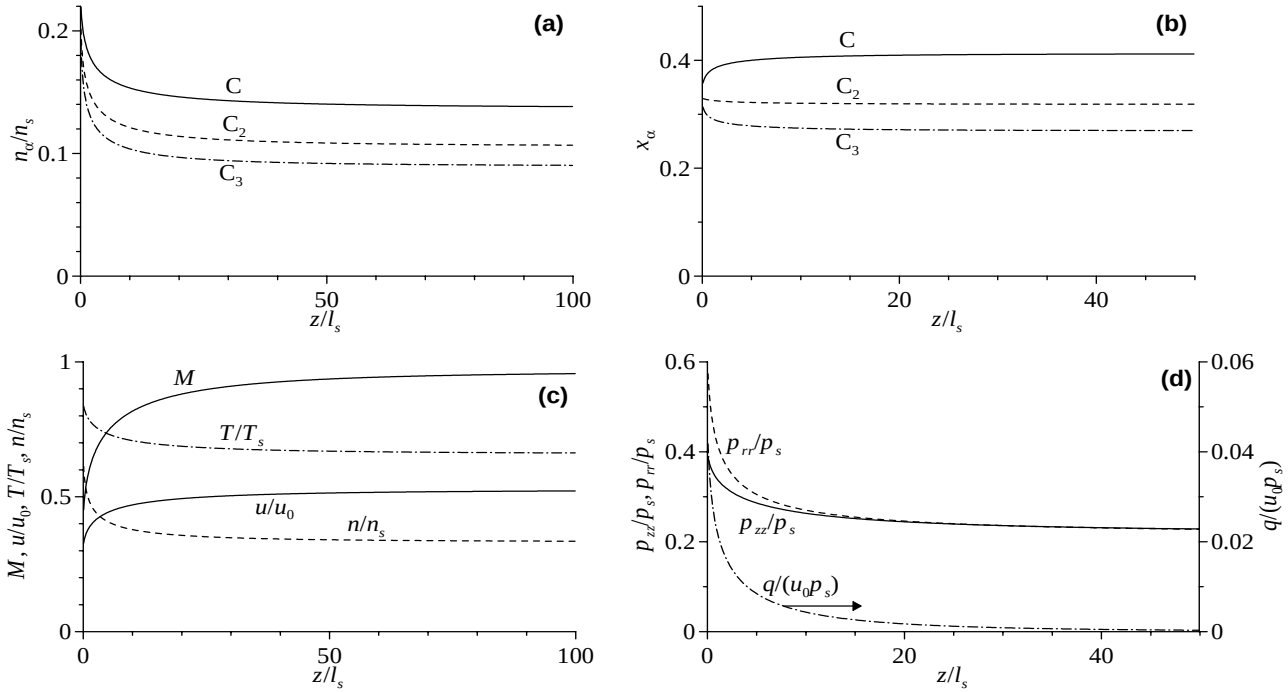

FIGURE 2. Distributions of dimensionless parameters in the Knudsen layer at pressure ratio $p_a/p_s = 0.22$ and equal saturated pressures of the components at the surface, $p_{s1} = p_{s2} = p_{s3} = p_s/3$: (a), dimensionless densities n_α/n_s of the components; (b), relative concentrations x_α of the components; (c), local Mach number M and dimensionless density, n/n_s, velocity, u/u_0, and temperature, T/T_s, of the mixture; (d), dimensionless components of the pressure tensor, p_{rr}/p_s and p_{zz}/p_s, and heat flow $q/(u_0p_s)$.

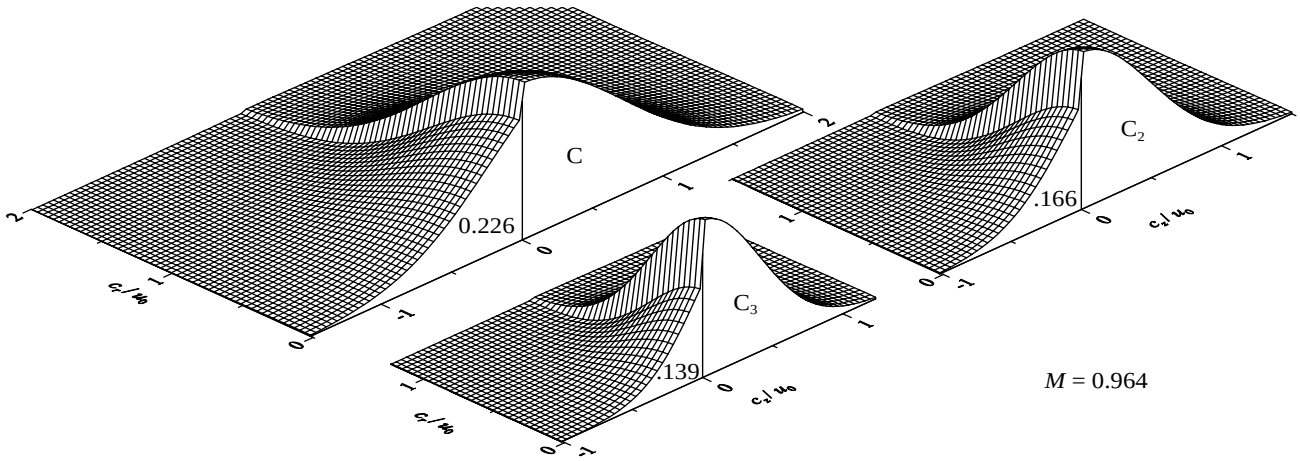

FIGURE 3. Velocity distributions (arbitrary units) of carbon species, C, C_2, and C_3, on the condensed phase surface at pressure ratio $p_a/p_s = 0.22$, Mach number $M = 0.964$, and equal saturated pressures of the components. Axial, c_z, and radial, c_r, molecular velocities are normalized with thermal velocity $u_0 = (2kT_s/m_1)^{1/2}$. Recondensation fraction is shown on each diagram.

Importance of the backward part of velocity distribution relative to the forward one decreases with molecular mass (see Fig. 3). This is in line with molecular collision mechanics: heavier molecules are rarely scattered to backward directions. The recondensation fractions of carbon species shown in Fig. 3 are calculated as ratios of backward molecular flux at $c_z < 0$ to forward flux at $c_z > 0$. Notice that the recondensation fraction in monatomic vapor at similar conditions, $M = 1$, is 0.185 [5]. Thus, fraction of atomic carbon backscattered in the Knudsen layer is higher than in one-component case and fractions of backscattered molecules C_2 and C_3 are less. The same tendency of increasing the recondensation fraction with molecular mass was observed for binary mixture [8].

Figure 4 shows calculations at different pressure ratios, p_a/p_s, between 0.22 and 1 that almost cover the entire range of Mach numbers from 0 to 1. The vapor characteristics in this figure are the same as in Fig. 2 but they refer to the region behind the Knudsen layer where there is no dependence on coordinate. Vapor temperature, T_a, and total number density, n_a, and pressure, p_a, of all the components are compared with the corresponding values for one-component vapor in Fig. 4 (a). It is noticeable that present multicomponent model (crosses) gives the same results as previous calculations (open and dark symbols) for the relaxation model in one-component case [6,11]. The difference is within numerical error. Similar conclusion was obtained for binary mixture [8].

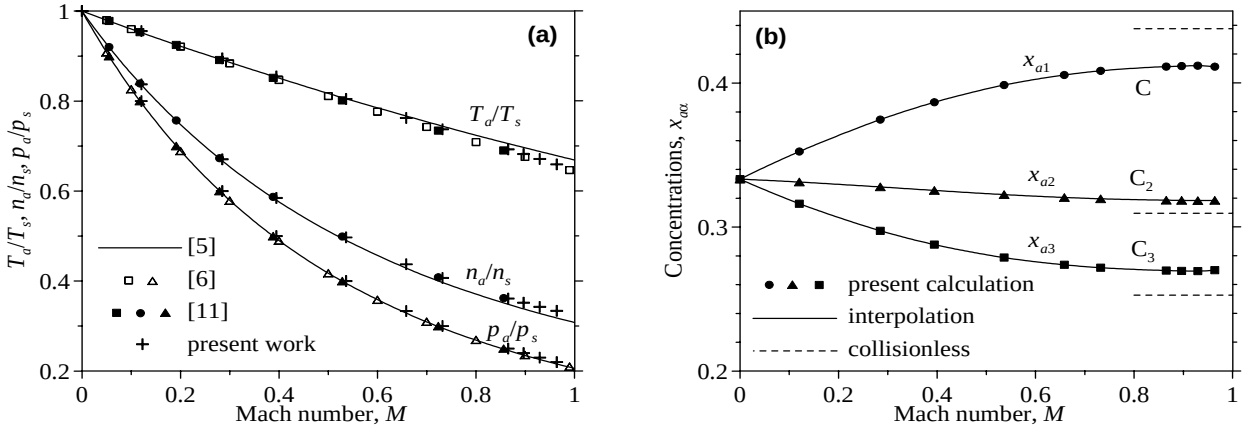

FIGURE 4. Carbon vapor parameters far from the surface as functions of the Mach number at equal partial pressures $p_{s1} = p_{s2} = p_{s3} = p_s/3$ in the saturated vapor. (a), comparison of temperature, T_a/T_s, density, n_a/n_s, and pressure, p_a/p_s, ratios for multicomponent carbon vapor (crosses) with those for one-component vapor: curves, analytical theory by Ytrehus [5]; open and dark symbols, numerical calculations for the relaxation model by Sone et al. [6] and by Gusarov et al. [11], respectively. (b), relative concentrations of carbon species, $x_{a\alpha}$: symbols, numerical results; full line curves, their spline interpolations; broken lines, collisionless evaporation (the Hertz-Knudsen equation).

Essential results concern molecular composition of carbon vapor presented in Fig. 4 (b). At low Mach numbers, $M << 1$, vapor composition is about the composition of the saturated vapor with $x_{a1} = x_{a2} = x_{a2} = 1/3$. Concentration of carbon atoms, x_{a1}, increases with the Mach number because of their higher thermal velocity relative to the molecules. However, x_{a1} does not attain the collisionless limit given by the Hertz-Knudsen evaporation low (upper broken line in Fig. 4 (b)). This appears to be due to the highest recondensation fraction of the atoms. On the contrary, concentrations of carbon molecules, C_2 and C_3, decrease with the Mach number tending to their collisionless limits (middle and lower broken lines) but do not attain them.

Thus, the molecular composition of carbon vapor is determined by two opposite tendencies: the first is decreasing the thermal velocity with molecular mass that leads to decreasing the concentration and the second is decreasing the recondensation fraction with molecular mass that leads to increasing the concentration. Actually, the first tendency is more important for the considered conditions, and so the concentration of carbon species decreases with their molecular mass.

The considered example of graphite evaporation at equal partial saturated pressures of C, C_2, and C_3 suggests a general conclusion that evaporation rate and vapor temperature do not depend on molecular composition of vapor and can be obtained from the well-known theory of one-component evaporation. On the other hand, the molecular composition itself may considerably differ from the composition of the saturated vapor and can be obtained using the present multicomponent kinetic model.

CONSLUSIONS

A numerical kinetic approach to gas mixtures is proposed which is based on a relaxation model for the Boltzmann equation. Strong evaporation of graphite with formation of a three-component vapor is analyzed at equal saturation pressures of atoms C and molecules C_2 and C_3.

The structure of a multicomponent Knudsen layer at strong evaporation is qualitatively the same as in the one-component case. However, molecular composition of the vapor changes through the Knudsen layer when the distance to the surface increases, and tends to a composition different from that of the saturated vapor.

Relations between the pressure and temperature ratios and the Mach number behind the Knudsen layer do not depend on vapor composition and are the same as in one-component vapor. The molecular composition of vapor is determined by decreasing the thermal velocity with molecular mass that decreases evaporation rate of heavier species and by decreasing the recondensation fraction with molecular mass that acts oppositely.

REFERENCES

1. Zavitsanos, P. D., and Carlson, G. A., "Experimental study of the sublimation of graphite at high temperatures," J. Chem. Phys. 59, 2966-2973 (1973).
2. Krajnovich, D., "Laser sputtering of highly oriented pyrolytic graphite at 248 nm," J. Chem. Phys. 102, 726-743 (1995).
3. Wakabayashi, T., Momose, T., and Shida, T., "Mass spectroscopic studies of laser ablated carbon clusters as studied by photoionization with 10.5 eV photons under high vacuum," J. Chem. Phys. 111, 6260-6263 (1999).
4. Kokai, F., Takahashi, K., Yudasaka, M., and Iijima, S., "Laser ablation of graphite-Co/Ni and growth of single-wall carbon nanotubes in vortexes formed in an Ar atmosphere," J. Phys. Chem. B 104, 6777-6784 (2000).
5. Ytrehus, T., "Theory and experiments on gas kinetics in evaporation," in Rarefied Gas Dynamics, edited by J.L. Potter, AIAA, New York, 1977, pp. 1197-1212.
6. Sone, Y., and Sugimoto, H., "Strong evaporation from a plane condensed phase," in Adiabatic Waves in Liquid-Vapor Systems, edited by G.E.A. Meier and P.A. Thompson, Springer, Berlin, 1990, pp. 293-304.
7. Sibold, D. and Urbassek, H., "Monte Carlo study of Knudsen layers in evaporation from elemental and binary media," Phys. Fluids A **5**, 243-256 (1993).
8. Frezzotti, A., "Kinetic theory description of the evaporation of multi-component substances," in Rarefied Gas Dynamics, edited by C. Shen, Peking University Press, Beijing, 1997, pp. 837-846.
9. Taguchi, S., Aoki, K., Takata, S., "Vapor flows condensing at incidence onto a plane condensed phase in the presence of a noncondensable gas. I. Subsonic condensation," Phys. Fluids 15, 689-705 (2003).
10. Garzo, V., Santos, A., and Brey, J.J., "A kinetic model for a multicomponent gas," Phys. Fluids A 1, 380-383 (1989).
11. Gusarov, A.V., and Smurov, I., "Gas-dynamic boundary conditions of evaporation and condensation: Numerical analysis of the Knudsen layer," Phys. of Fluids 14, 4242-4255 (2002).
12. Peric-Radic, J., Romelt, J., Peyerimhoff, S. D., and Buenker, R. J., "Configuration interaction calculation of the potential curves for the C_3 molecule in its ground and lowest-lying Π_u states," Chem. Phys. Lett. 50, 344-350 (1977).